

WINTER POLAR WARMINGS AND THE MERIDIONAL TRANSPORT ON MARS SIMULATED WITH A GCM.

A.S. Medvedev, P. Hartogh, T. Kuroda, *Max-Planck-Institute for Solar System Research, Katlenburg-Lindau, 37191, Germany (medvedev@mps.mpg.de).*

Introduction

We present a series of numerical experiments with the recently developed general circulation model of the Martian atmosphere (MAOAM) to examine the relative role of the mechanical and diabatic forcing on the meridional circulation. Magnitudes and locations of winter polar warmings are determined by the strength and the poleward extent of this circulation, rather than directly by the radiative heating. This work was partly motivated by the polar temperatures simulated with MAOAM, which appear to be warmer than in other Martian GCMs. Given the paucity of measurements above 50-60 km, these GCM experiments provide insight on the nature of the circulation in the middle atmosphere of Mars: whether it primarily is induced thermally by the differential heating (Hadley cell), or driven mechanically by breaking/dissipating waves (“extratropical pump”), as on Earth.

Experiment design

In all the numerical experiments described below, the model was spun up from the state of the rest and the globally uniform temperature $T = 160$ K. The spin-up was performed for the perpetual Northern summer corresponding to the fixed solar longitude $L_s = 90^\circ$. After 15 days of the integration time, the simulated fields achieve a practically equilibrium state as determined from the total kinetic energy. If not otherwise explicitly stated, the diurnal cycle was allowed in the simulations. The results presented below represent snapshots at the end of the integration period.

The 4 experiments are presented here:

- Control run with full physics.
- Run with inhibited eddies. Non-zonal Newtonian cooling was applied to artificially reduce eddies in the model.
- Run with the flat topography and no diurnal variations. This setup virtually removes planetary waves generated by the flow over topography, and the thermal tide.
- Run with the dust load increased 10-fold: from 0.05 to 0.5.

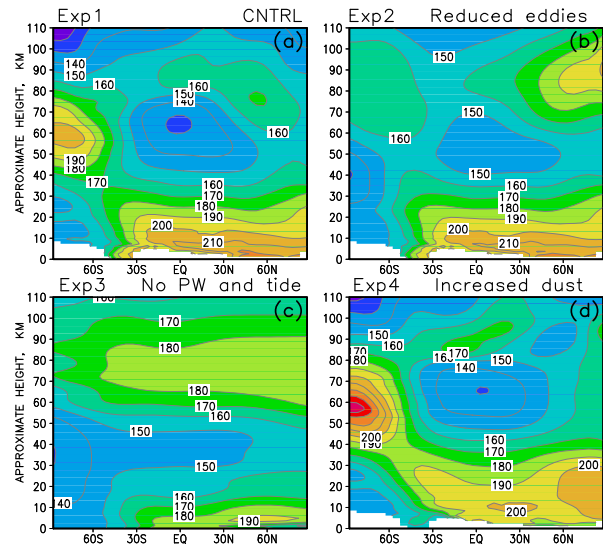


Figure 1: Zonal mean temperature for $L_s = 90^\circ$ in 4 sensitivity experiments.

Eddy forcing of the meridional circulation

This effect enters the mean zonal momentum equation in the Transformed Eulerian Mean (TEM) formulation through the divergence of the Eliassen-Palm (EP) fluxes [Andrews *et al.*, 1987]:

$$\bar{u}_t + \bar{v}^* [(a \cos \phi)^{-1} (\bar{u} \cos \phi)_\phi - f] + \bar{w}^* \bar{u}_z = (\rho_0 a \cos \phi)^{-1} \nabla \cdot F. \quad (1)$$

In (1), \bar{v}^* and \bar{w}^* are the residual velocities, ϕ is the latitude, f is the Coriolis parameter, and F is the EP flux. The latter is plotted in Figure 2a. To show the induced meridional transport, we plotted the stream lines of the residual circulation in Figure 2c. The residual velocities take into account the transport by eddies, and represent the net transport closer than the Eulerian counterparts. The meridional component of the residual velocity \bar{v}^* is shown in Figure 2b. Its magnitude of several tens m s^{-1} is significantly stronger than that on the Earth, and is in line with the results from other Martian GCMs. The transience in (1) can be neglected for the seasonal average. Therefore, \bar{v}^* may be determined from (1) from the EP flux divergence and the advection. Figure 2d presents the estimate for \bar{v}^* calculated using the eddy forcing from the panel 2a, and the Coriolis term: $\bar{v}^* \approx -(f \rho_0 a \cos \phi)^{-1} \nabla \cdot F$. Comparison with the Figure 2b shows that the residual meridional velocity \bar{v}^* is

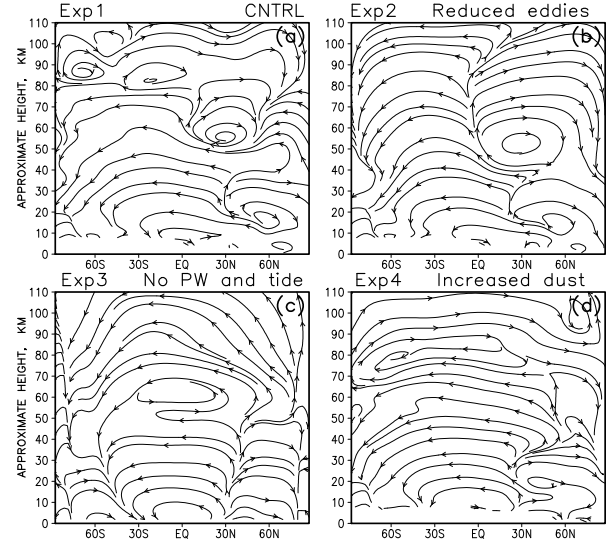


Figure 3: Residual streamfunction simulated in 4 sensitivity experiments.

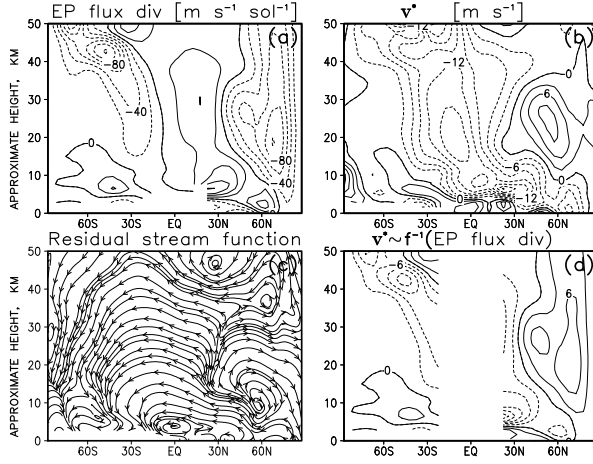


Figure 2: The fields simulated for the solar longitude $L_s = 90^\circ$: a) Eliassen-Palm flux divergence, the contour interval is $100 \text{ m s}^{-1} \text{ sol}^{-1}$; b) the residual meridional velocity \bar{v}^* ; c) The residual stream function; and d) the estimate of the meridional residual velocity from (1): $\bar{v}^* \approx -f^{-1}(\rho_0 a \cos \phi)^{-1} \nabla \cdot F$

determined largely by the EP flux divergence (at least in mid- to high latitudes). In other words, the meridional transport is forced primarily by the eddies, and the peculiarities of this forcing control the winter polar warming.

Conclusions

In all but Exp3 we found that the circulation is forced primarily by the mechanical effects of dissipating eddies. Only in Exp3 the meridional transport was reminiscent to the thermally-induced Hadley circulation. Therefore, generation, propagation, breaking and/or dissipation of planetary waves and solar tides, and their interaction with the mean flow should be properly resolved in GCMs.

In Exp4, the winter polar warming is not the direct result of heating due to the increased absorption of the solar radiation by dust, but is caused by the extension of the meridional transport cell poleward [Wilson, 1997]. More close examination shows the mechanism of the poleward extension of the meridional cell. Strengthened westerly polar jet (prograde winds) causes the planetary waves and tides propagate more vertically and prevent from dissipation at lower levels. EP fluxes are then converge stronger near the upper edge of the polar vortex, and create stronger EP flux divergence. The latter intensifies the meridional circulation and increases the polar temperature maximum.

High sensitivity of the circulation above $\approx 80 \text{ km}$ may be an indication of missing effects in our and other GCMs. The potential candidate is the gravity wave drag exerted by broad-spectrum waves. Further measurements of large scale wind and temperature fields in the upper atmosphere as well as the statistics for small scale fluctuations will help to constrain models and GWD parameterizations.